UC Davis

UC Davis Previously Published Works

Title

Put Your Backbone into It: Excited-State Structural Relaxation of PffBT4T-2DT Conducting Polymer in Solution

Permalink

https://escholarship.org/uc/item/7q8147zs

Journal

The Journal of Physical Chemistry C, 122(12)

ISSN

1932-7447

Authors

Dantanarayana, Varuni
Fuzell, Jack
Nai, Dingqi
et al.

Publication Date

2018-03-29

DOI

10.1021/acs.jpcc.8b01356

Peer reviewed

eScholarship.org Powered by the California Digital Library
University of California

THE JOURNAL OF PHYSICAL CHEMISTRY C

Article

Cite This: J. Phys. Chem. C 2018, 122, 7020−7026

pubs.acs.org/JPCC

Put Your Backbone into It: Excited-State Structural Relaxation of PffBT4T-2DT Conducting Polymer in Solution

Varuni Dantanarayana,[†,∥] Jack Fuzell,[†,∥] Dingqi Nai,[‡] Ian E. Jacobs,[‡,⊥] He Yan,[§] Roland Faller,[‡] Delmar Larsen,[†,*] and Adam J. Moule[‡,*]

[†]Department of Chemistry, University of California, Davis 95616, United States

[‡]Department of Materials Science and Engineering, University of California, Davis 95616, California, United States

[§]Department of Chemistry and Hong Kong Branch of Chinese National Engineering Research Center for Tissue Restoration and Reconstruction, Hong Kong University of Science and Technology (HKUST), Clear Water Bay, Kowloon, Hong Kong

Supporting Information

ABSTRACT: Conformational and energetic disorder in organic semiconductors reduces charge and exciton transport because of the structural defects, thus reducing the efficiency in devices such as organic photovoltaics and organic light-emitting diodes. The main structural heterogeneity is because of the twisting of the polymer backbone that occurs even in polymers that are mostly crystalline. Here, we explore the relationship between polymer backbone twisting and exciton delocalization by means of transient absorption spectroscopy and density functional theory calculations. We study the PffBT4T-2DT polymer which has exhibited even higher device efficiency with nonfullerene acceptors than the current record breaking PCE11 polymer. We determine the driving force for planarization of a polymer chain caused by excitation. The methodology is generally applicable and demonstrates a higher penalty for nonplanar structures in the excited state than in the ground state. This study highlights the morphological and electronic changes in conjugated polymers that are brought about by excitation.

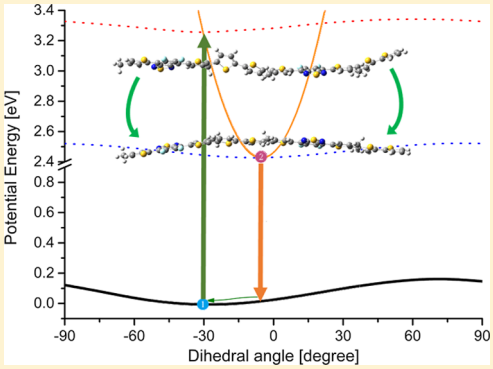

INTRODUCTION

The primary photodynamics of organic semiconductors (OSCs) has been intensely studied over the last two decades in organic photovoltaics (OPV) and other opto-electronic devices.[1−6] The efficiency of such devices depends on a strong understanding of how material choice and design affect device function.[6−8] Even though conjugated polymers in OSCs have been extensively investigated, the mechanism for efficient exciton transport which is crucial for high device efficiency is still not properly understood. Conformational and energetic disorder in conjugated polymers reduces charge-transport efficiency by providing energetic traps that localize the charge carriers because of extensive heterogeneity. A main source of this heterogeneity is the twisting of polymer backbones around rotatable bonds between planar building blocks which occurs even in polymers that are mostly crystalline.[9,10] Thus, exploring the relationship between exciton delocalization and the behavior of the polymer backbone structure in picoseconds after excitation of a polymer is of particular interest.

Previously,[11] we studied the photophysics of the conjugated polymer poly(3-hexylthiophene-2,5-diyl) (P3HT) in solution. We found that coiled P3HT planarizes rapidly (∼2 ps) upon excitation. The timescale for returning to a coiled state after return to the ground state was an order of magnitude greater (∼20 ps). This planarization of the polymer backbone in the excited state was monitored by observing the red shift of the stimulated emission (SE) as a function of time after the excitation pulse in a transient absorption (TA) spectroscopy experiment. Other groups have observed excited-state planarization in numerous other conjugated polymers using ultrafast spectroscopy.[4,11−20] We now quantify the driving force for the planarization of a conjugated polymer chain in the presence of an exciton.

PffBT4T-2DT (Figure 1a) was selected for our case study because of the large changes in the ground-state delocalization as a function of dihedral disorder along the polymer backbone.[21] PffBT4T-2DT has the same backbone structure, but longer alkyl chains and less crystallinity than poly[(5,6-difluoro-2,1,3-benzothiadiazol-4,7-diyl)-*alt*-(3,3-di(2-octyldodecyl)-2,2′; 5′,2″; 5″,2‴-quaterthiophen-5,5-diyl)] (PffBT4T-2OD), the OPV record-breaking polymer discovered by Yan et al.[21] PffBT4T-2DT has been shown to deliver even higher OPV efficiency with nonfullerene acceptors than PffBT4T-2OD (PCE11).[22] Here, we demonstrate that the excited-state dynamics of the polymer in solution gives a reasonably simple

Received: February 7, 2018
Revised: February 22, 2018
Published: February 23, 2018

ACS Publications © 2018 American Chemical Society

DOI: 10.1021/acs.jpcc.8b01356
J. Phys. Chem. C 2018, 122, 7020−7026

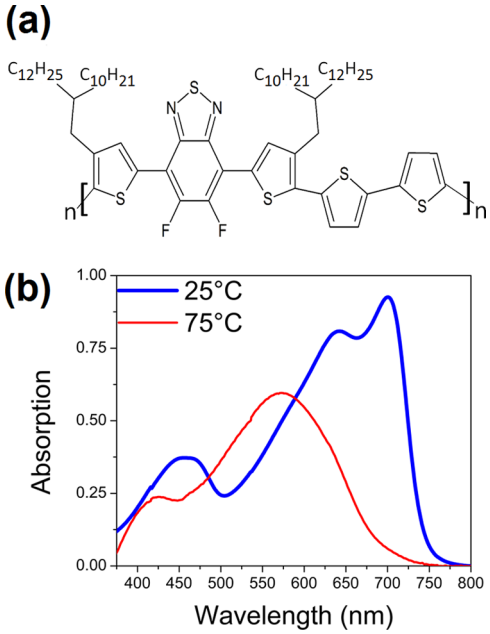

Figure 1. (a) Chemical structure of PffBT4T-2DT and (b) static spectra of PffBT4T-2DT at 25 °C (blue) and 75 °C (red).

probe of the coupling between the exciton and structural order in a conjugated polymer.

We present the first full TA spectroscopy data of pure PffBT4T-2DT in solution at two temperatures, 25 and 75 °C, with an excitation wavelength of 400 nm and a broadband probe that covers the visible and near IR spectrum. To interpret these TA spectroscopy data, we use ab initio density functional theory (DFT)[23,24] to calculate the ground-state energy manifold as a function of dihedral angle rotation along the polymer backbone as well as time-dependent DFT (TD-DFT)[25] to calculate the excited-state energy as a function of the polymer configuration for both coiled and relaxed (planar) geometries of a PffBT4T-2DT dimer. Not many comparisons between excited-state DFT and TD-DFT calculations on conjugated polymers have been presented previously.[26−28] Here, we calculate and discuss the accurate way of computing the molecular geometries and electronic energies involved in a vertical excitation under a rigid rotational scan and use these calculations to develop structurally sensitive potential energy landscapes for both ground and excited states.

EXPERIMENTAL AND COMPUTATIONAL METHODS

Spectroscopy. The PffBT4T-2DT sample was dissolved in dichlorobenzene, and TA signals were collected in experiments at 25 and 75 °C. The temperature measurements were performed starting with low temperatures on the same day in back-to-back measurements. For the temperature control, the PffBT4T-2DT sample was kept at 25 and 75 °C using a Fisher Scientific Isotemp 1016D recirculating heat bath and a homemade glass sample holder. Before the data were collected, the sample was circulated at the set temperature for 15 min to ensure equilibration. The PffBT4T-2DT samples were excited with 400 nm pulses created by doubling the fundamental output of our Spectra-Physics Spitfire titanium sapphire laser. The probe pulse was formed by focusing the 800 nm fundamental pulses into a slowly moving 2 mm calcium fluoride disk; the signals were collected with a 256 pixel silicon array. The evolution-associated difference spectra (EADS) were calculated using CarpetView spectroscopy data analysis software.

Computational Methods. DFT calculations were performed on the PffBT4T dimer in vacuum. Bulky alkyl chains are mainly used as a solubilizing group in PffBT4T-2DT[29] substituted with methyl groups for computational economy. The optimized geometries and the energies were calculated using the Gaussian 09 package.[30] The structures were fully optimized in the ground-state and first-excited-state energies at the 6-311G(d,p) basis set level. The subsequent potential energy calculations in ground-state calculations were performed with the 6-31G/B3LYP functional (the Becke 3 and the Lee−Yang−Parr hybrid functional) and the lowest excited singlet state with the TD-DFT approach and 6-31G/CAM-B3LYP functional (B3LYP with Coulomb attenuating method).[31] This particular basis set was chosen as a compromise between high computational cost and quality of the theoretical calculation. The long-range Coulomb-attenuated B3LYP functional, CAM-B3LYP, has proven to be more accurate when predicting excited-state energies.[32] Furthermore, a rigid potential energy surface (PES) around the dihedral angle with the lowest torsional energy was calculated to get the vertical excitation energy to the first-excited singlet state. We realize that even though there are effects (e.g., polymer molecular weight, longer alkyl chain substituent, level of theory, solvent effects, and temperature effects) which tend to affect the exact energy levels that are not considered in these theoretical calculations, it is possible to obtain valuable information by comparing calculations of the same or similar types.

RESULTS AND DISCUSSION

Ground-State Spectra and Polymer Conformation. Many thiophene-based conjugated systems exhibit large solvochromic and thermochromic shifts associated with the dihedral disorder along the polymer backbone.[33] PffBT4T-2DT also shows strong thermochromism in solution; therefore, varying the solution temperature affects the aggregation and backbone structure. We use the solution temperature to control the polymer configuration and then probe the ultrafast photodynamics of aggregated and unaggregated morphologies. The static absorption spectra of PffBT4T-2DT at 25 °C (blue curve) and 75 °C (red curve) are compared in Figure 1b. Both of the static spectra match the temperature-dependent static spectra reported previously for PffBT4T-2OD.[21] The vibronic peaks at 650 and 700 nm in the 25 °C spectrum show[34] that PffBT4T-2DT forms aggregates of planar chains,[8] allowing strong delocalization of the ground-state wave function along the backbone. According to the Spano model,[35] the presence of J-aggregate characteristics indicates that individual polymer chains are highly planar with weak intermolecular coupling between chains. This means that at 25 °C, the PffBT4T-2DT chain is constrained to be planar but that the ground-state wave function is not delocalized across multiple chains. The polymer can be treated as a single planar molecule. At 75 °C, the absorption spectrum exhibits broad peaks centered at 410 and 560 nm, corresponding to high structural heterogeneity and localized ground-state wave functions. This verifies that at higher temperatures, the polymers in solution are single-coiled chains which disrupts the conjugation along the polymer backbone.[21] Thus, the polymer strands are less constrained and more mobile, which allows for the polymer strand to change its conformation when excited and minimizing its free energy.

DOI: 10.1021/acs.jpcc.8b01356
J. Phys. Chem. C 2018, 122, 7020−7026

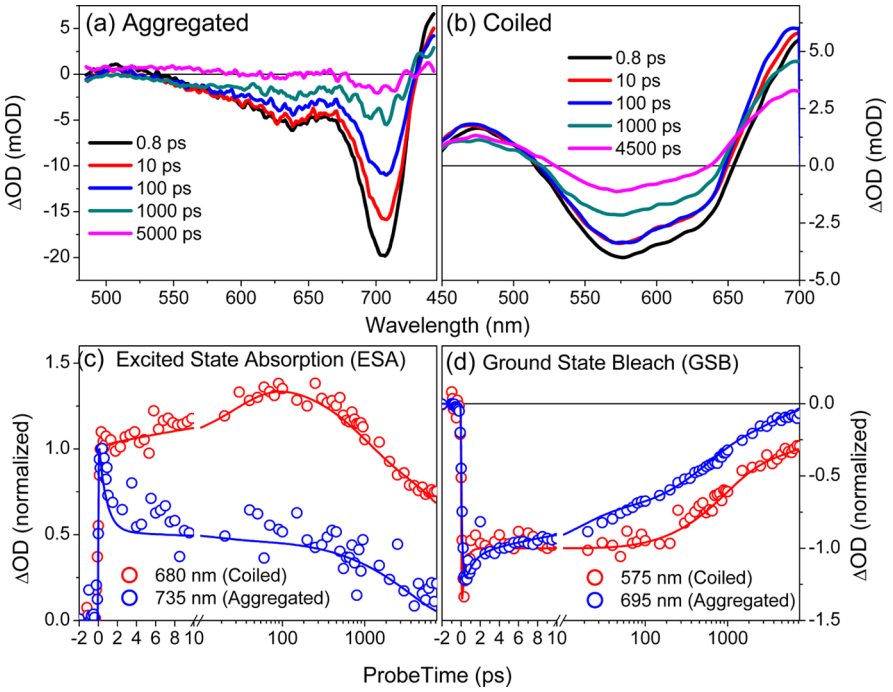

Figure 2. TA spectra at selected time points after 400 nm excitation for both (a) 25 °C (aggregated) and (b) 75 °C (coiled). Note the different spectral windows between the two panels. Kinetics showing (c) ESA and (d) GSB of PffBT4T-2DT at 25 °C (aggregated) and 75 °C (coiled). Note, in the kinetic plots, the linear to logarithmic transition in the plots at 10 ps.

TA Spectroscopy and Excited-State Dynamics. Figure 2a,b shows TA spectra of PffBT4T-2DT dissolved in chlorobenzene at 25 and 75 °C, respectively. Both sets of spectra are dominated by the ground-state bleach (GSB), the large negative signal from ∼525 to ∼725 nm in the 25 °C sample and from ∼510 to ∼650 nm in the 75 °C sample that represent the depopulation of the ground state by the excitation pulse. Positive excited-state absorption (ESA) bands are located on the red side at >725 nm in the aggregated 25 °C sample and at >650 nm in the coiled 75 °C sample. Furthermore, there are additional ESA bands on the blue side of the spectra with peaks at 510 nm in the 25 °C sample and at 475 nm in the 75 °C sample. The 75 °C solution excited-state bands are blue-shifted compared to the 25 °C solution (Figure 2), similar to their respective spectral features in the ground-state spectra (Figure 1b). This blue-shifting can be attributed to polymer strands being less aggregated in the 75 °C sample. In Figure 2a,b, the blue and red ESA bands exhibit near identical decay kinetics (Supporting Information Figure S1), which indicate that we only have one visible, initially excited-state population at each temperature. Given that there is no spectral evolution of either ESA in the first few picoseconds, they must represent the spectral signature of the singlet exciton in PffBT4T-2DT.[13] If the excited polymer does form polarons, they occur faster than our temporal resolution (≈100 fs). In comparison with other polymers in solution (e.g., P3HT),[11] PffBT4T-2DT does not exhibit clear SE near its primary absorption band in either the 25 °C or the 75 °C solution.

The excited-state kinetics is strongly dependent on the polymer configuration. For the solutions at both temperatures, the excited-state kinetics (Figure 2c,d) was fit using multi-wavelength global analysis.[36] The kinetic data for each solution were fit using a set of four EADS (Supporting Information Figure S2): EADS are fixed spectra that evolve into each other on certain time scales to fit the data, where each of the fixed EADS corresponds to the TA spectrum of the raw data in the given time frame. Ignoring the early time (<1 ps) decay because of exciton annihilation caused by the high-incident fluence of the excitation pulse, the GSB (Figure 2d) is flat for ≃100 ps before the decay back to the ground state begins in the coiled 75 °C sample (red curve), whereas decay of the GSB to the ground state begins immediately in the aggregated 25 °C sample (blue curve). This is due to the difference in localization effects as seen in other polymers:[5,37,38] localized excitons move by hopping and are slower than delocalized excitons that can sample larger regions of the polymer and begin to decay almost immediately. The longest decay constant in the 25 °C solution is 3.6 ns (blue curve in Figure 2d), whereas the longest decay constant in the 75 °C solution (red curve in Figure 2d) cannot be determined because of the time range of our experimental setup (>7.5 ns).

The two solutions differ in another important way: both ESA and GSB for the aggregated 25 °C solution (blue curve in Figure 2c,d, respectively) decay monotonically, whereas in the coiled 75 °C solution (red curve in Figure 2c,d, respectively) the absorption on the red side of Figure 2b (≃630 to >700 nm) shows an increase in the signal on a 30 ps time scale. This secondary increase is attributed to a spectral blue shift of the ESA peak in the 75 °C sample.

Previously, when we measured P3HT in methanol where the SE red-shifts on a 2 ps timescale,[11] it was attributed to the planarization of the polymer backbone in the excited state. Other thiophene-based polymers, such as oligothiophenes[14] and poly[3-(2,5-dioctylp-henyl)thiophene],[39] exhibit similar behavior on comparable time scales, 46 and 15 ps, respectively. Thus, we attribute this spectral shift to the planarization of the PffBT4T-2DT backbone in the excited state. Although SE shifting is generally used to identify backbone planarization in TA spectroscopy measurements,[11] we do not observe SE over our measured wavelength because of an overlapping ESA band.

DOI: 10.1021/acs.jpcc.8b01356
J. Phys. Chem. C 2018, 122, 7020−7026

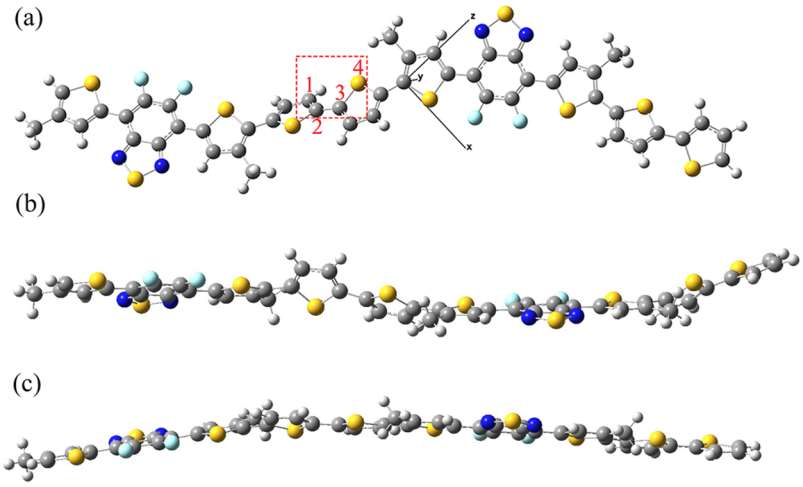

Figure 3. (a) Molecular geometry of the optimized structure of the PffBT4T-2DT dimer. Labeled atoms in the red box denote the dihedral angle around which the rigid rotational PES is calculated. Side views of the optimized geometry of the (b) ground state and (c) first excited state of the PffBT4T-2DT dimer. Color scheme: gray C atoms, yellow S atoms, teal F atoms, blue N atoms, and white H atoms.

Instead, we utilize the blue-shifting of the peak of the red-side ESA. This absorption band blue-shifts because the occupied excited-state energy level relaxes, increasing the gap between itself and the higher-lying unoccupied excited states. It is possible for intersystem crossing (ISC) to occur in conjugated polymers and for triplet excitons to form on this 30 ps time scale.[16] However, if singlet excitons were transitioning to triplet excitons, there would be a decrease in the initially populated ESA bands, which we do not observe.

Other options for describing the ~33 ps spectrum blue shift in the 75 °C sample are triplet exciton formation or some form of excited-state charge transfer. Generally, the charge transfer in a polymer carries with it a signature in the NIR spectrum, where multiple states with different decay rates will be visible.[40,41] In our data (Supporting Information Figure S3), the NIR spectra do not show multiple populations as the entire spectrum decays with the same time constants (Supporting Information Figure S2). Therefore it seems that the charge transfer is not a good explanation. As the sample was not measured both with and without O_2, we are not able to rule out definitively that the spectral blue shift is caused by triplet exciton formation. However, we do not believe this to be the case because both the formation time (~33 ps) and the decay time (nanosecond scale) are too fast in general to be ascribed to triplet excitons. Triplet excitons that form through ISC in polymers such as P3HT or PTB7 form on the nanosecond timescale[40,42] and they decay on the microsecond timescale, not the nanosecond timescale that we observe for the resulting excited state after the blueshift.[43,44]

Simulating Excited-State Energies and Conformations. We performed a full geometry optimization on a model PffBT4T dimer (Figure 3a) in two different energy configurations. We replaced the full $C_{24}H_{49}$ side chain in PffBT4T-2DT by a methyl group for the computational efficiency. The ground-state geometry was optimized using DFT/B3LYP[45] (Figure 3b) and the first excited-singlet-state geometry (Figure 3c) using TD-DFT/CAM-B3LYP[31] (see the Supporting Information for computational details). All simulations were performed with Gaussian 0930 using the 6-311G(d,p) basis set. It can be seen from these optimized structures that the lowest energy configuration for the ground state exhibits variations of the dihedral angles (Table S1) along the backbone, whereas the lowest energy structure in the excited state is planar (Figure 3a,b, respectively), similar to P3HT in solution[11] The fluorine atoms reduce the torsional angle of the polymer backbone because of the high electron-withdrawing capability of fluorine and strong attraction between the fluorine and sulfur on the adjacent thiophene.[46] We observe that the backbone is flat on either side of the fluorine-substituted benzothiadiazole unit in, both, the ground and the first excited states. The alkyl side chains, in contrast, tend to cause an increase in the dihedral disorder of the polymer backbone.[47] A systematic study of side chain branching shows that branching at the C_2 position combined with long side chains leads to thin-film polymers with low dihedral disorder and high charge mobilities as exhibited in PffBT4T-2DT.[48,49] We can infer that if our PffBT4T model included longer alkyl chain substituents, then the dihedral angles would be even more coiled in the ground state than that found here. Additionally, from the bond-length analysis (Supporting Information Table S2), we see that the PffBT4T dimer exhibits shorter single bonds and longer double bonds along the conjugated backbone upon excitation, corresponding to stronger conjugation than that in the ground state. This is a strong indication for higher-charge delocalization in the first excited state.

To identify which backbone dihedral has the lowest rotation barrier in solution, we calculated the rotational potential energy around each of the nine dihedral angles along the dimer backbone (Supporting Information Figure S3). The calculations were performed by rotating each dihedral by a small angle in both directions from the equilibrium ground-state geometry and then computing the average energy for each dihedral angle. The dihedral angle that is easiest to rotate (lowest torsional potential) is between the two unsubstituted thiophene rings depicted by a red box in Figure 3a. The subsequent detailed rigid torsional potential calculations were, for computational efficiency, performed exclusively around this angle, using the 6-31G basis set at the level of theory mentioned above.

We calculated the excitation energy (ΔE_{vert}) for each ground-state configuration as a function of the dihedral angle around this easiest-to-rotate bond. We performed rigid rotational scans, that is, calculated the single-point energies for every 15° of

DOI: 10.1021/acs.jpcc.8b01356
J. Phys. Chem. C 2018, 122, 7020−7026

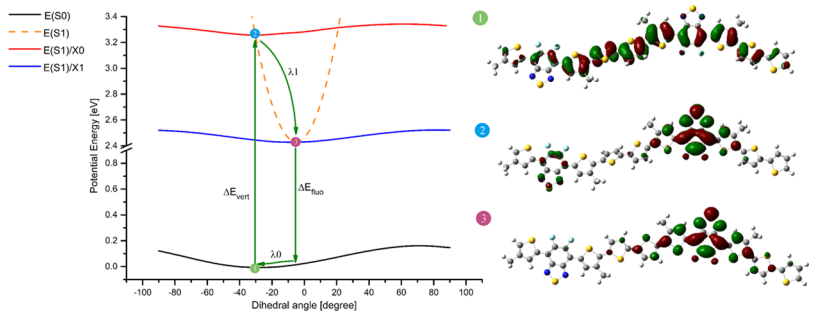

Figure 4. Rotational PESs for PffBT4T dimer. $E(S0)$ and $E(S1)/X0$ depict the ground-state and excited-state energies, respectively, in the ground-state optimized geometry, whereas $E(S1)/X1$ is the excited-state energy around the optimized excited-state geometry. The dashed line $E(S1)$ indicates the excited-state energy curve, after instantaneous vertical excitation from the ground-state optimized geometry (point 1 to point 2) and fast relaxation to point 3 within the excited-state energy manifold. Contour plots of the molecular orbitals for the ground-state HOMO energy and excited-state LUMO energy, respectively, in the optimized ground-state geometry (points 1 and 2) and optimized excited-state LUMO energy level (point 3).

rotation around the dihedral angle covering the range of −90° to +90° while maintaining all other bond lengths and angles at the values of the equilibrium geometry. These vertical transitions are depicted in Figure 4. Although this calculation does not reproduce the full ground-state PES, it introduces significant structural disorder and allows understanding of the effect of dihedral disorder on the excited-state relaxation dynamics.

The vertical transition represented by ΔE_{vert} (point (1) to (2) in Figure 4) corresponds to the instantaneous electronic charge transfer while the nuclei are still in their ground-state geometry. Thus

$$\Delta E_{vert} = E(S1, X0) - E(S0)$$

where $E(S0)$ (Figure 4 black curve) is the ground-state energy and $E(S1,X0)$ (Figure 4 red curve) is the first singlet-excited-state energy at the ground-state equilibrium geometry, X0. After the vertical transition to the excited state, the molecule will rapidly relax to the energy-minimized excited-state geometry, X1, depicted as point (3) Figure 4. This excited-state relaxation is driven by the reorganization energy (point (2) to (3) in Figure 4)

$$\lambda 1 = E(S1, X0) - E(S1, X1)$$

and follows the pathway shown by the potential energy curve labeled $E(S1)$ under harmonic approximation in Figure 4.

We calculated $E(S1,X0)$ (Figure 4 red curve) and $E(S1,X1)$ (Figure 4 blue curve) by determining the excited-state energy at the ground-state equilibrium geometry and excited-state equilibrium geometry, respectively, as a function of the rigid rotation around the easiest-to-rotate dihedral in Figure 3a around the minimized geometry of the excited state. $E(S1)$ (Figure 4 dashed line) represents the excited-state energy surface, which encompasses the electronic energy change and nuclear rearrangement. This curve was obtained by coupling the vertical transition point and excited state minimum after structural relaxation. Naturally, a different $E(S1)$ exists for each ground-state configuration where each $E(S1)$ relaxes to the same X1 configuration.

Similarly, fluorescence from the excited state to the ground state corresponds to

$$\Delta E_{fluo} = E(S1, X1) - E(S0, X1)$$

Finally, the molecule can relax back to the ground-state minimized geometry with reorganization energy

$$\lambda 0 = E(S0, X1) - E(S0, X0)$$

The molecular orbital contour plots for $E(S0)$, $E(S1,X1)$, and $E(S1,X1)$ are depicted in Figure 4. The electron density transfers from $E(S0)$ highest occupied molecular orbital (HOMO) to $E(S1,X0)$ lowest unoccupied molecular orbital (LUMO) in the E_{vert} transition. Clearly, the $E(S1,X0)$ wave function is strongly localized because of the dihedral disorder in the polymer backbone. When $E(S1,X0)$ relaxes to $E(S1,X1)$ LUMO, the dihedral disorder is removed and the wave function delocalizes over more polymer subunits.

This series of calculations shows that $\lambda 1 \gg \lambda 0$ for all molecular configurations, which is why the excited-state relaxation is rapid and the ground-state relaxation is comparatively slow. It can be observed that although the excited-state PES (S1) shows a deep well (Figure 4 dashed line), the ground-state energy profile (S0) is quite flat, indicating that the molecule in its planar excited state is significantly stiffer than in the coiled ground state. We posit that $\lambda 1$ will be much larger than $\lambda 0$ for all conjugated polymers in solution and that the experimental and theoretical methodology presented here constitutes a systematic way to compare the effect of molecular geometry on the excited-state reorganization energy in conjugated polymers.

CONCLUSIONS

In conclusion, ultrafast TA spectroscopy was performed on PffBT4T-2DT solutions at 25 and 75 °C corresponding to planar and coiled backbone configurations. In addition, the ground-state DFT and excited-state TD-DFT calculations were carried out on the ground-state and first-singlet excited-state of the PffBT4T-2DT dimer. The TA spectroscopy data showed that at 25 °C, the sample has a predominantly planar aggregated polymer configuration even in the ground state. The exciton is immediately delocalized without the need for relaxation of the polymer chain to a planar configuration. Thus, the decay back to the ground state starts right away. In comparison, at 75 °C, the polymer is in a coiled unaggregated state and has a localized exciton. To minimize the energy of the exciton, the polymer chain quickly relaxes to a planar configuration, which delocalizes the exciton causing its ESA to blue shift. Once the polymer is locally planarized, the exciton decays to the ground state. The kinetics of the coiled polymer showed that they planarize in the excited state on the picosecond timescale. This interpretation was supported by

DOI: 10.1021/acs.jpcc.8b01356
J. Phys. Chem. C 2018, 122, 7020−7026

the DFT and TD-DFT calculations where we found that the PffBT4T-2DT dimer is coiled in the ground state and becomes planar and exhibits a higher degree of conjugation in its first-singlet excited state. Within the Franck−Condon principle, we have accurately calculated the excited state energy along with the geometrical changes. In addition, we showed that the excited-state relaxation energy is, in general, much higher than the ground-state relaxation energy and thereby provides a driving force for planarization in the excited state because of the presence of the exciton. The calculation of this driving force over a variety of configurations suggests that the energetic driving force to planarize the polymer backbone in the excited state is a general feature of the conjugated polymers.

■ ASSOCIATED CONTENT

Supporting Information

The Supporting Information is available free of charge on the ACS Publications website at DOI: 10.1021/acs.jpcc.8b01356.

Decay kinetics, difference spectra, TA spectra, DFT optimized geometry parameters, DFT calculated torsion potential, and Mulliken charges (PDF)

■ AUTHOR INFORMATION

Corresponding Authors

*E-mail: dlarsen@ucdavis.edu. Phone: +1 (530) 204-8319 (D.L.).

*E-mail: amoule@ucdavis.edu. Phone: +1 (530) 754-8669 (A.J.M.).

ORCID

Ian E. Jacobs: 0000-0002-1535-4608

He Yan: 0000-0003-1780-8308

Roland Faller: 0000-0001-9946-3846

Delmar Larsen: 0000-0003-4522-2689

Present Address

[⊥]Cavendish Laboratory, University of Cambridge, Cambridge, UK.

Author Contributions

[∥]V.D. and J.F. contributed equally to this work.

Notes

The authors declare no competing financial interest.

■ ACKNOWLEDGMENTS

The authors acknowledge Dr. Mikas Vengris from Light Conversion Ltd. for donating the global analysis software package. This project was carried out with funding from the U.S. Department of Energy, Office of Basic Energy Sciences, Division of Materials Sciences and Engineering, under Award DE-SC0010419 to AM and from the National Science Foundation (DMR-1035468) to DSL. We thank the Hong Kong Innovation and Technology Commission for support through projects ITC-CNERC14SC01 and ITS/083/15.

■ REFERENCES

(1) Facchetti, A. π-Conjugated Polymers for Organic Electronics and Photovoltaic Cell Applications. *Chem. Mater.* **2011**, *23*, 733−758.

(2) Burroughes, J. H.; Bradley, D. D. C.; Brown, A. R.; Marks, R. N.; Mackay, K.; Friend, R. H.; Burns, P. L.; Holmes, A. B. Light-emitting Diodes Based on Conjugated Polymers. *Nature* **1990**, *347*, 539−541.

(3) Friend, R. H.; Gymer, R. W.; Holmes, A. B.; Burroughes, J. H.; Marks, R. N.; Taliani, C.; Bradley, D. D. C.; Santos, D. A. D.; Brédas, J. L.; Lögdlund, M.; et al. Electroluminescence in Conjugated Polymers. *Nature* **1999**, *397*, 121.

(4) Tretiak, S.; Saxena, A.; Martin, R. L.; Bishop, A. R. Conformational Dynamics of Photoexcited Conjugated Molecules. *Phys. Rev. Lett.* **2002**, *89*, 097402.

(5) Kaake, L. G.; Moses, D.; Heeger, A. J. Coherence and Uncertainty in Nanostructured Organic Photovoltaics. *J. Phys. Chem. Lett.* **2013**, *4*, 2264−2268.

(6) Xin, G.; Baumgarten, M.; Müllen, K. Designing π-Conjugated Polymers for Organic Electronics. *Prog. Polym. Sci.* **2013**, *38*, 1832−1908.

(7) Vogelbaum, H. S.; Sauvé, G. Recently Developed High-Efficiency Organic Photoactive Materials for Printable Photovoltaic Cells: A Mini Review. *Synth. Met.* **2017**, *223*, 107−121.

(8) Arias, A. C.; MacKenzie, J. D.; McCulloch, I.; Rivnay, J.; Salleo, A. Materials and Applications for Large Area Electronics: Solution-Based Approaches. *Chem. Rev.* **2010**, *110*, 3−24.

(9) Venkateshvaran, D.; Nikolka, M.; Sadhanala, A.; Lemaur, V.; Zelazny, M.; Kepa, M.; Hurhangee, M.; Kronemeijer, A. J.; Pecunia, V.; Nasrallah, I.; et al. Approaching Disorder-Free Transport in High-Mobility Conjugated Polymers. *Nature* **2014**, *515*, 384−388.

(10) Korovyanko, O. J.; Österbacka, R.; Jiang, X. M.; Vardeny, Z. V.; Janssen, R. A. J. Photoexcitation Dynamics in Regioregular and Regiorandom Polythiophene Films. *Phys. Rev. B: Condens. Matter Mater. Phys.* **2001**, *64*, 235122.

(11) Busby, E.; Carroll, E. C.; Chinn, E. M.; Chang, L.; Moulé, A. J.; Larsen, D. S. Excited-State Self-Trapping and Ground-State Relaxation Dynamics in Poly(3-hexylthiophene) Resolved with Broadband Pump−Dump−Probe Spectroscopy. *J. Phys. Chem. Lett.* **2011**, *2*, 2764−2769.

(12) Park, K. H.; Kim, P.; Kim, W.; Shimizu, H.; Han, M.; Sim, E.; Iyoda, M.; Kim, D. Excited-State Dynamic Planarization of Cyclic Oligothiophenes in the Vicinity of a Ring-to-Linear Excitonic Behavioral Turning Point. *Angew. Chem., Int. Ed. Engl.* **2015**, *54*, 12711−12715.

(13) Guo, J.; Ohkita, H.; Benten, H.; Ito, S. Near-IR Femtosecond Transient Absorption Spectroscopy of Ultrafast Polaron and Triplet Exciton Formation in Polythiophene Films with Different Regioregularities. *J. Am. Chem. Soc.* **2009**, *131*, 16869−16880.

(14) Kim, P.; Park, K. H.; Kim, W.; Tamachi, T.; Iyoda, M.; Kim, D. Relationship between Dynamic Planarization Processes and Exciton Delocalization in Cyclic Oligothiophenes. *J. Phys. Chem. Lett.* **2015**, *6*, 451−456.

(15) Gallaher, J. K.; Chen, K.; Huff, G. S.; Prasad, S. K. K.; Gordon, K. C.; Hodgkiss, J. M. Evolution of Nonmirror Image Fluorescence Spectra in Conjugated Polymers and Oligomers. *J. Phys. Chem. Lett.* **2016**, *7*, 3307−3312.

(16) Yu, W.; Donohoo-Vallett, P. J.; Zhou, J.; Bragg, A. E. Ultrafast Photo-Induced Nuclear Relaxation of a Conformationally Disordered Conjugated Polymer Probed with Transient Absorption and Femtosecond Stimulated Raman Spectroscopies. *J. Chem. Phys.* **2014**, *141*, 044201.

(17) Yu, W.; Zhou, J.; Bragg, A. E. Exciton Conformational Dynamics of Poly(3-hexylthiophene) (P3HT) in Solution from Time-Resolved Resonant-Raman Spectroscopy. *J. Phys. Chem. Lett.* **2012**, *3*, 1321−1328.

(18) Zhou, J.; Yu, W.; Bragg, A. E. Structural Relaxation of Photoexcited Quaterthiophenes Probed with Vibrational Specificity. *J. Phys. Chem. Lett.* **2015**, *6*, 3496−3502.

(19) Chang, M.-H.; Hoffmann, M.; Anderson, H. L.; Herz, L. M. Dynamics of Excited-State Conformational Relaxation and Electronic Delocalization in Conjugated Porphyrin Oligomers. *J. Am. Chem. Soc.* **2008**, *130*, 10171−10178.

(20) Parkinson, P.; Müller, C.; Stingelin, N.; Johnston, M. B.; Herz, L. M. Role of Ultrafast Torsional Relaxation in the Emission from Polythiophene Aggregates. *J. Phys. Chem. Lett.* **2010**, *1*, 2788−2792.

(21) Liu, Y.; Zhao, J.; Li, Z.; Mu, C.; Ma, W.; Hu, H.; Jiang, K.; Lin, H.; Ade, H.; Yan, H. Aggregation and Morphology Control Enables

Multiple Cases of High-Efficiency Polymer Solar Cells. *Nat. Commun.* **2014**, *5*, 5293.
(22) Li, Z.; Jiang, K.; Yang, G.; Lai, J. Y. L.; Ma, T.; Zhao, J.; Ma, W.; Yan, H. Donor Polymer Design Enables Efficient Non-Fullerene Organic Solar Cells. *Nat. Commun.* **2016**, *7*, 13094.
(23) Parr, R. G. *Density Functional Theory of Atoms and Molecules. Horizons of Quantum Chemistry: Proceedings of the Third International Congress of Quantum Chemistry*; Springer: Kyoto, Japan, 1980; pp 5−15.
(24) Becke, A. D. Density-Functional Thermochemistry. III. The Role of Exact Exchange. *J. Chem. Phys.* **1993**, *98*, 5648−5652.
(25) Runge, E.; Gross, E. K. U. Density-Functional Theory for Time-Dependent Systems. *Phys. Rev. Lett.* **1984**, *52*, 997.
(26) Adamo, C.; Jacquemin, D. The Calculations of Excited-State Properties with Time-Dependent Density Functional Theory. *Chem. Soc. Rev.* **2013**, *42*, 845.
(27) Brause, R.; Krügler, D.; Schmitt, M.; Kleinermanns, K.; Nakajima, A.; Miller, T. A. Determination of the Excited-State Structure of 7-Azaindole-Water Cluster using a Franck-Condon Analysis. *J. Chem. Phys.* **2005**, *123*, 224311.
(28) Hlel, A.; Mabrouk, A.; Chemek, M.; Khalifa, I. B.; Alimi, K. A DFT Study of Charge-Transfer and Opto-Electronic Properties of Some New Materials Involving Carbazole Units. *Comput. Condens. Matter* **2015**, *3*, 30−40.
(29) Sen, C. P.; Valiyaveettil, S. Synthesis and Structure-Property Investigation of Multi-Arm Oligothiophenes. *RSC Adv.* **2015**, *5*, 105435−105445.
(30) Frisch, M. J.; Trucks, G. W.; Schlegel, H. B.; Scuseria, G. E.; Robb, M. A.; Cheeseman, J. R.; Scalmani, G.; Barone, V.; Petersson, G. A.; Nakatsuji, H.; et al. *Gaussian 09*, Revision B.01; Gaussian, Inc.: Wallingford CT, 2016.
(31) Yanai, T.; Tew, D. P.; Handy, N. C. A New Hybrid Exchange−Correlation Functional Using the Coulomb-Attenuating Method (CAM-B3LYP). *Chem. Phys. Lett.* **2004**, *393*, 51−57.
(32) Bouzzine, S. M.; Salgado-Morán, G.; Hamidi, M.; Bouachrine, M.; Pacheco, A. G.; Glossman-Mitnik, D. DFT Study on Polythiophene Energy Band Gap and Substitution Effects. *J. Chem.* **2015**, *2015*, 1−12.
(33) Bouman, M. M.; Havinga, E. E.; Janssen, R. A. J.; Meijer, E. W. Chiroptical Properties of Regioregular Chiral Polythiophenes. *Mol. Cryst. Liq. Cryst. Sci. Technol., Sect. A* **1994**, *256*, 439−448.
(34) Martin, T. P.; Wise, A. J.; Busby, E.; Gao, J.; Roehling, J. D.; Ford, M. J.; Larsen, D. S.; Moulé, A. J.; Grey, J. K. Packing Dependent Electronic Coupling in Single Poly(3-hexylthiophene) H- and J-Aggregate Nanofibers. *J. Phys. Chem. B* **2013**, *117*, 4478−4487.
(35) Spano, F. C. The Spectral Signatures of Frenkel Polarons in H- and J-Aggregates. *Acc. Chem. Res.* **2010**, *43*, 429−439.
(36) van Stokkum, I. H. M.; Larsen, D. S.; van Grondelle, R. Global and Target Analysis of Time-Resolved Spectra. *Biochim. Biophys. Acta, Bioenerg.* **2004**, *1657*, 82−104.
(37) Batista, E. R.; Martin, R. L. Exciton Localization in a Pt-Acetylide Complex. *J. Phys. Chem. A* **2005**, *109*, 9856−9859.
(38) Schwartz, B. J.; Nguyen, T.-Q.; Wu, J.; Tolbert, S. H. Interchain and Intrachain Exciton Transport in Conjugated Polymers: Ultrafast Studies of Energy Migration in Aligned MEH-PPV/mesoporous Silica Composites. *Synth. Met.* **2001**, *116*, 35−40.
(39) Westenhoff, S.; Beenken, W. J. D.; Friend, R. H.; Greenham, N. C.; Yartsev, A.; Sundström, V. Anomalous Energy Transfer Dynamics due to Torsional Relaxation in a Conjugated Polymer. *Phys. Rev. Lett.* **2006**, *97*, 166804.
(40) Guo, J.; Ohkita, H.; Benten, H.; Ito, S. Near-IR Femtosecond Transient Absorption Spectroscopy of Ultrafast Polaron and Triplet Exciton Formation in Polythiophene Films with Different Regioregularities. *J. Am. Chem. Soc.* **2009**, *131*, 16869−16880.
(41) Szarko, J. M.; Rolczynski, B. S.; Lou, S. J.; Xu, T.; Strzalka, J.; Marks, T. J.; Yu, L.; Chen, L. X. Photovoltaic Function and Exciton/Charge Transfer Dynamics in a Highly Efficient Semiconducting Copolymer. *Adv. Funct. Mater.* **2014**, *24*, 10−26.
(42) Kraus, H.; Heiber, M. C.; Väth, S.; Kern, J.; Deibel, C.; Sperlich, A.; Dyakonov, V. Analysis of Triplet Exciton Loss Pathways in PTB7:PC71BM Bulk Heterojunction Solar Cells. *Sci. Rep.* **2016**, *6*, 29158.
(43) Ohkita, H.; Cook, S.; Astuti, Y.; Duffy, W.; Heeney, M.; Tierney, S.; McCulloch, I.; Bradley, D. D. C.; Durrant, J. R. Radical Ion Pair Mediated Triplet Formation in Polymer-Fullerene Blend Films. *Chem. Commun.* **2006**, 3939−3941.
(44) Chow, P. C. Y.; Gélinas, S.; Rao, A.; Friend, R. H. Quantitative Bimolecular Recombination in Organic Photovoltaics through Triplet Exciton Formation. *J. Am. Chem. Soc.* **2014**, *136*, 3424−3429.
(45) Lee, C.; Yang, W.; Parr, R. G. Development of the Colle-Salvetti Correlation-Energy Formula Into a Functional of the Electron Density. *Phys. Rev. B: Condens. Matter Mater. Phys.* **1988**, *37*, 785.
(46) Zhang, A.; Xiao, C.; Wu, Y.; Li, C.; Ji, Y.; Li, L.; Hu, W.; Wang, Z.; Ma, W.; Li, W. Effect of Fluorination on Molecular Orientation of Conjugated Polymers in High Performance Field-Effect Transistors. *Macromolecules* **2016**, *49*, 6431.
(47) Bredas, J.; Heeger, A. Theoretical Investigation of Gas-Phase Torsion Potentials along Conjugated Polymer Backbones: Polyacetylene, Polydiacetylene, and Polythiophene. *Macromolecules* **1990**, *23*, 1150.
(48) Meager, I.; Ashraf, R. S.; Mollinger, S.; Schroeder, B. C.; Bronstein, H.; Beatrup, D.; Vezie, M. S.; Kirchartz, T.; Salleo, A.; Nelson, J.; et al. Photocurrent Enhancement from Diketopyrrolopyrrole Polymer Solar Cells through Alkyl-Chain Branching Point Manipulation. *J. Am. Chem. Soc.* **2013**, *135*, 11537−11540.
(49) Zhang, F.; Hu, Y.; Schuettfort, T.; Di, C.-a.; Gao, X.; McNeill, C. R.; Thomsen, L.; Mannsfeld, S. C. B.; Yuan, W.; Sirringhaus, H.; et al. Critical Role of Alkyl Chain Branching of Organic Semiconductors in Enabling Solution-Processed N-Channel Organic Thin-Film Transistors with Mobility of up to 3.50 cm(2) V-1 s(-1). *J. Am. Chem. Soc.* **2013**, *135*, 2338−2349.

DOI: 10.1021/acs.jpcc.8b01356
J. Phys. Chem. C 2018, 122, 7020−7026